Type-II intermittency in a coupled nonlinear oscillator: Experimental observation

Jung-Yun Huang and Jong-Jean Kim*
Physics Department, Korea Advanced Institute of Science and Technology, P.O. Box 150 Chongyangni, Seoul 131, Korea
(Received 3 September 1986)

Observation of the type-II Pomeau-Manneville intermittency was realized in a coupled nonlinear oscillator circuit employing a *p-n* junction diode and linear oscillator elements. It seems that Hopf bifurcation and period tripling are among the most important precursors to the type-II intermittency. Experimental results are found to agree very well with the numerical results derived from the coupled discrete maps of Pomeau-Manneville.

Recent studies in nonlinear oscillators have brought a new understanding to the dynamic structures of nature, i.e., how they can be driven into chaos from order.[1] A simple nonlinear oscillator with only a few degrees of freedom shows very complicated dynamics and, in general, reaches a chaotic state when the nonlinearity control parameter is increased. Most nonlinear dynamic systems are well explained by simple discrete maps[2] employing only one or two parameters which measure the nonlinearity of the system, as exemplified by many experimental results.[3] It is well known that there are at least three distinctive routes to chaos, one of which is Pomeau-Manneville's "intermittency."[4] The intermittency is characterized by chaotic bursts which appear stochastically in between regular (laminar) states. As a parameter—which measures the distance from the critical point where chaotic bursts begin to appear—is increased, laminar periods decrease continuously, leading to total chaos as in the second-order transition. Pomeau and Manneville classified the intermittency into three types according to the eigenvalues of the transfer function of the Poincaré return map. Although type-I and type-III intermittencies are well studied in both theory and experiments,[5] type-II intermittency has not been reported yet in experimental studies.[6]

We want to report here our first observation of type-II intermittency in a coupled oscillator circuit composed of a *p-n* junction diode (IN4004), and linear electrical elements. The circuit is shown in Fig. 1. One can easily obtain circuit equations for the circuit of Fig. 1 by use of Kirchhoff's laws:

$$L(\ddot{Q}_1+\ddot{Q}_2)+R(\dot{Q}_1+\dot{Q}_2)+V_d(Q_2)=V_0\cos(\omega_1 t)\ , \quad (1a)$$

$$L_1\ddot{Q}_1+R_1\dot{Q}_1+Q_1/C_1-V_d(Q_2)=0\ , \quad (1b)$$

where L (2.0 mH) and L_1 (3.2 mH) are linear inductors, R_1 (12.2Ω) represents the dc resistance of L_1, and R (1.2Ω+50Ω) represents the serial sum of the dc resistance of L and the 50Ω output impedance of the oscillator (Wavetek 142). C_1 (330 pF) is a ceramic capacitor and V_d represents the voltage drop across the diode. At $V_0=4.25$ V and $\omega_1=45$ kHz, the circuit current i was 9.33 mA. Two-frequency oscillation on a torus can be excited in this circuit by the driving signal $V_0\cos(\omega_1 t)$: one oscillation with the drive frequency ω_1 and the other corresponding to the natural frequency of the closed loop circuit. Competitive interactions may then exist between the two oscillations yielding phase lockings and quasiperiodic signals.[7] Indeed the system has also shown a phase-locking fine structure in (ω_1, V_0) space, though we will confine our discussion to the region where type-II intermittency was observed. This novel observation was made at relatively low frequencies of 40–50 kHz as compared with the characteristic frequencies above 100 kHz showing the well-known nonlinear responses in the nonlinear *RCL* circuit. V_c was sampled with a fast sample-and-hold circuit [the (ω_1, V_0) space diagram was very similar to that of V_d]. Periods of sampling pulses were synchronized with those of the driving signals. To study the (V_{n+p}, V_n) return map or the $(V_n, V_{n+p}, V_{n+2p}, \ldots)$ time sequences, for example, we sampled signals at every pth period of driving signals by employing a frequency-divider circuit and the signals were displayed on an oscilloscope. Sampling points were adjusted to get the best stable signals (usually the peak values were sampled).

The type-II intermittency was observed in conjunction with a Hopf bifurcation as well as a period tripling, i.e., there were three spirals growing and whorling out of the ghosts of the fixed points (source point) with different phases and spread into the chaotic repellers around each

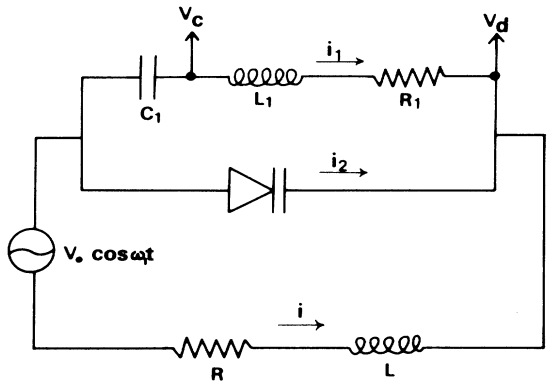

FIG. 1. Circuit diagram used in the experiment. The *p-n* junction diode is denoted here as accompanying nonlinear capacitance.

source point [see Figs. 2(b) and 3(a)] as ω_1 or V_0 was slightly increased near critical values. In the laminar phases the attractor visits each of the three spirals alternatively, leading to the period tripling. In order to trace the same spiral, signals were sampled at every third period as shown in Fig. 2(c). Here one should note that figures displayed on the oscilloscope are not (r_n,t) or (r_{n+1},r_n) but $[X_n\ (=r_n\cos\theta_n),t]$ and (X_{n+1},X_n) where r_n corresponds to V_n. To distinguish the spiraling behavior of the type-II intermittency, a few data points were retained from Fig. 2(c) and deconvoluted by the modulation frequency to get (r_n,t) from (X_n,t). A stroboscopy of the spiral is shown in Fig. 3(a). The temporal signal appears as if the amplitudes are modulated at the frequency ω_2 $(\approx\omega_1/15)$ with the modulation amplitude growing simultaneously until it becomes a chaotic burst and loses its stability. After chaotic bursts the signal returns again to the laminar phase with arbitrary initial amplitude, i.e., the attractors are reinjected at random points in the laminar region of the return map. One can see clearly in Fig. 2(c) that the larger the initial amplitude, the shorter the length of the laminar periods. When an attractor is reinjected into a laminar region, it rides on any one of the three spirals, i.e., it hops randomly between spirals, which may contribute to the low-frequency $1/f$-noise characteristic of the intermittency, though the stochastic distribution of the laminar lengths may be responsible for the major part of the noise.[8]

Pomeau-Manneville's type-II intermittency can be modeled by coupled discrete maps in polar coordinates as[9]

$$r_{n+1}=f(r_n)=(1+\epsilon)r_n+ur_n^3\ , \tag{2a}$$

$$\theta_{n+1}=g(\theta_n)=\theta_n+\Omega\ , \tag{2b}$$

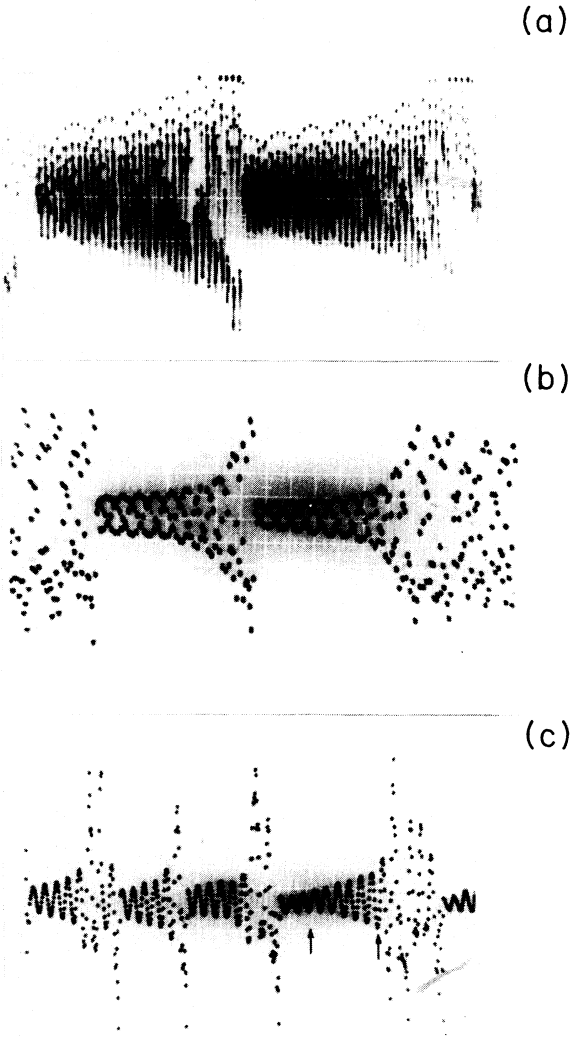

FIG. 2. Type-II intermittency signals at $V_0=4.4$ V and (ω_1). Unless noted, x: 5 ms/div, y: 2V/div. (a) A snapshot of the real signal: only peaks are displayed (45.025 kHz), x: 0.5 ms/div. (b) When the signal is sampled at the frequency ω_1, it appears as three spirals winding around each other. Each point indicates peak value of the real signal (44.956 kHz); x: 1 ms/div. (c) A signal sampled at every third period: data points between arrows were used to obtain Fig. 3(a) (4.3 V, 45.020 kHz).

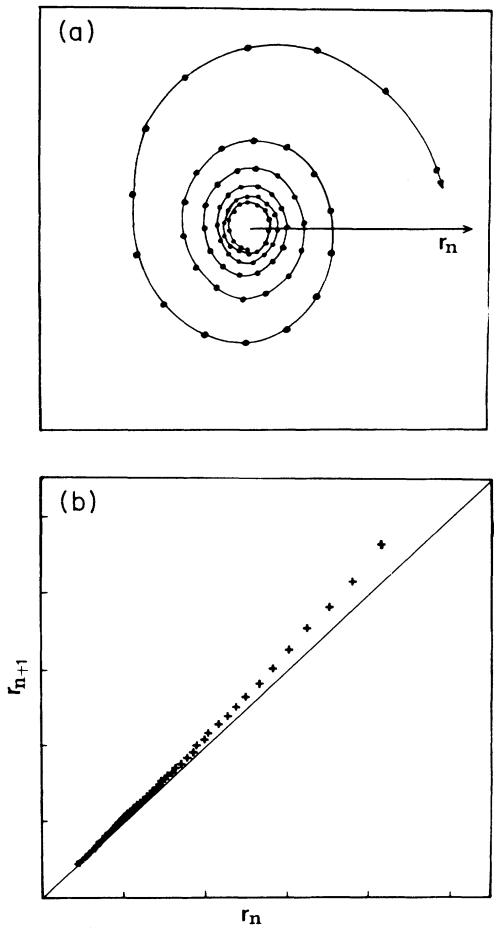

FIG. 3. (a) A spiral event corresponding to the time series of Fig. 2(c). Spiral frequency is taken to be $2\pi/15$ (see the text). (b) (r_{n+1},r_n) Poincaré map corresponding to (a). Least-square fit to Eq. (2a) gives $\epsilon=0.034$.

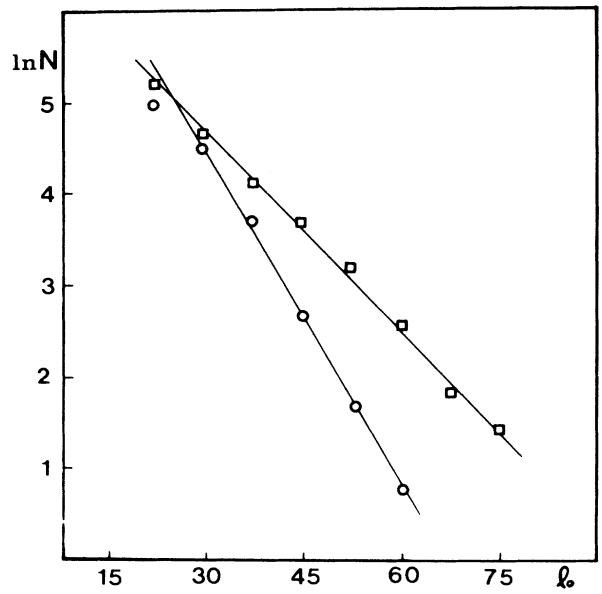

FIG. 4. Number of laminar periods with length greater than l_0. Least-squares fitting with Eq. (4) gives $\epsilon=0.039$. Straight lines are for visual guides. □, 45.020 kHz, 4.3 V; ○, 45.021 kHz, 4.5 V.

where Ω is the modulation (spiraling) frequency. The (r_{n+1}, r_n) return map was obtained from the experimental data [Fig. 2(c)] which gives the best fitting at $\epsilon=0.034$ as shown in Fig. 3(b). We could easily reproduce a similar signal to that of Fig. 2(c) using Eqs. (2a) and (2b) with parameter values of $\epsilon=0.034$, and $u=0.45$ as obtained from the experimental data. Ω was chosen as $2\pi/15$ to obtain the same modulation frequency $\omega_1/15$ of Fig. 2(c). A linear map was taken as a chaotic repeller to assume uniform reinjection probability.[10]

We consider another result characteristic of the type-II intermittency, the distribution of the length l of laminar periods. l depends on the reinjection points in the return map: As the attractor is reinjected closer to the origin, the longer the laminar period becomes. Assuming the reinjection probability is independent of the reinjection point, the probability $P(l_0)$ that the laminar length will be longer than l_0 becomes[11]

$$P(l_0) \propto \frac{\epsilon^2 e^{-2\epsilon l_0}}{(1-e^{-2\epsilon l_0})^2} \tag{3}$$

Then the cumulative distribution $N(l_0)$ is, by integration,

$$N(l_0) = \int_{l_0}^{\infty} P(l)dl \propto \frac{\epsilon^3 e^{-2\epsilon l_0}}{1-e^{-2\epsilon l_0}} . \tag{4}$$

The experimental data from 50 snapshots of intermittency signals with fixed parameters were used to plot $\ln N(l_0)$ versus l_0 at two different states corresponding to 172 (denoted by squares) and 153 (circles) laminar events, respectively, as shown in Fig. 4. Each step takes three periods of the driving signal. If we assume $\epsilon \gtrsim 0.034$, a typical experiment situation, we have $\epsilon l_0 \gtrsim 1$ and $\ln N(l_0)$ may well be approximated by a straight line with respect to l_0. This also agrees very well with experimental observations as can be seen in Fig. 4. The best fitting of the data (squares) with Eq. (4) gives $\epsilon=0.039$ which agrees well with the value obtained from the return map.

In summary, we have first observed the type-II intermittency, which is one of the important routes to chaos, in a nonlinear coupled oscillator simulator. The experimental observations could be explained fairly well in accordance with the results of the return maps. Our coupled oscillator has successfully exhibited various signals of nonlinear dynamics; notably it shows all three types of intermittencies in different (ω_1, V_0) sections of the parameter space as well as the Ruelle-Takens scenario[9] and period-doubling cascades.

*To whom correspondence should be addressed.

[1]*Proceedings of the International Conference on Order in Chaos, Los Alamos, 1982,* edited by D. Campbell and H. Rose [Physica **7D**, 1 (1983)]; and see Ref. 9.

[2]M. J. Feigenbaum, J. Stat. Phys. **19**, 25 (1978); J. P. Crutchfield, J. D. Farmer, and B. A. Huberman, Phys. Rep. **92**, 45 (1982).

[3]P. S. Linsay, Phys. Rev. Lett. **47**, 1349 (1981); J. C. Roux, Physica **7D**, 57 (1983); and see Ref. 5.

[4]P. Manneville and Y. Pomeau, Phys. Lett. **75A**, 1 (1979); Y. Pomeau and P. Manneville, Commun. Math. Phys. **74**, 189 (1980).

[5]Type-III intermittency was reported in a hydrodynamic system by M. Dubois, M. A. Rubio, and P. Berge, Phys. Rev. Lett. **51**, 1446 (1983).

[6]There is a recent report on the observation of the type-II intermittency in a periodically driven nonlinear oscillator equation: P. Richetti, F. Argoul, and A. Arneodo, Phys. Rev. A **34**, 726 (1986).

[7]M. H. Jensen, P. Bak, and T. Bohr, Phys. Rev. A **30**, 1960 (1984).

[8]I. Procaccia and H. Schuster, Phys. Rev. A **28**, 1210 (1983).

[9]H. G. Schuster, *Deterministic Chaos* (Physik-Verlag, Weinheim, 1984), Chap. 4.

[10]In Ref. 6, the authors reported that the reinjection probability may not be uniform.

[11]P. Manneville, J. Phys. (Paris) **41**, 1235 (1980); and see Ref. 9.

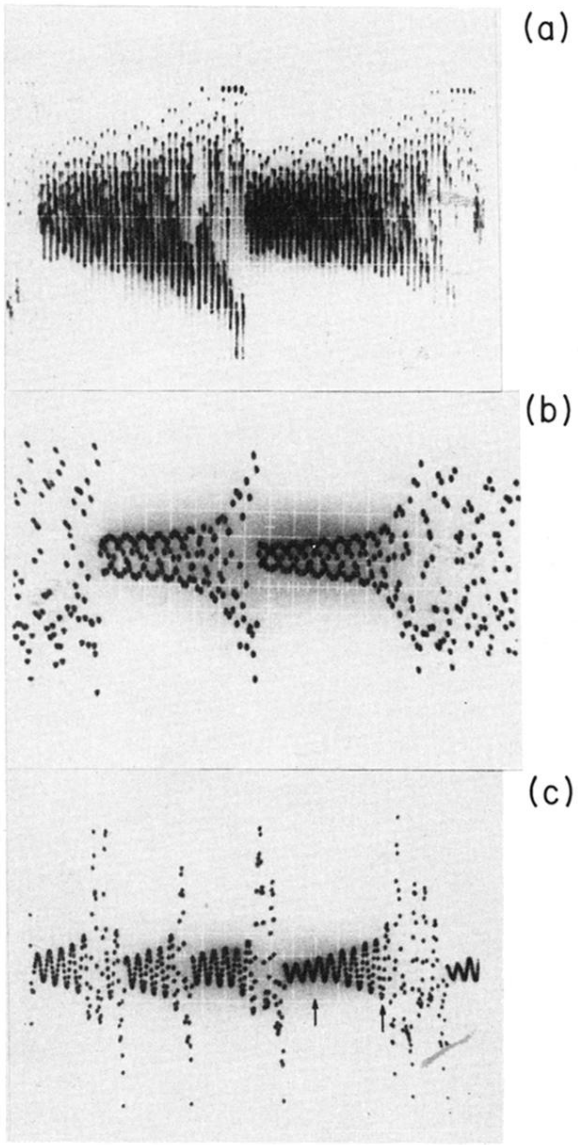

FIG. 2. Type-II intermittency signals at $V_0=4.4$ V and (ω_1). Unless noted, x: 5 ms/div, y: 2V/div. (a) A snapshot of the real signal: only peaks are displayed (45.025 kHz), x: 0.5 ms/div. (b) When the signal is sampled at the frequency ω_1, it appears as three spirals winding around each other. Each point indicates peak value of the real signal (44.956 kHz); x: 1 ms/div. (c) A signal sampled at every third period: data points between arrows were used to obtain Fig. 3(a) (4.3 V, 45.020 kHz).